2011 IEEE/RSJ International Conference on
Intelligent Robots and Systems
September 25-30, 2011. San Francisco, CA, USA

Human Swarm Modeling in Exhibition Space and Space Design

Masafumi Okada, Yuichi Motegi and Ko Yamamoto

***Abstract*— In an exhibition space, it is possible to control human flow implicitly by changing a layout of exhibits. The objectives of this paper are the layout optimization of exhibits to reduce congestion and the amenity space design. For these purposes, macro modeling of human swarm behavior and the optimization method of a layout of exhibits are required. So far, human swarm behavior has been modeled by two-dimensional vector field and individual behavior is represented by dynamics including collision avoidance vector of individuals. In this paper, we extend the human model to multi-dimensional dynamics in order to represent individual characteristics in measured data and visitors' stopping to view exhibits. In addition, a layout of exhibits is optimized based on the proposed model by minimizing collision avoidance vector. The proposed method is verified by simulations and experiments using swarm robots which consist of autonomous mobile robots and radio controlled robots. The results show that the comfortable exhibition space is designed.**

I. INTRODUCTION

An exhibition space such as an art museum is generally a crowded place. Visitors feel uncomfortable due to congestion, and it sometimes causes a serious accident. Reducing congestion helps with designing a comfortable and safe space. One of the methods of congestion reduction is redesigning and widen the exhibition space. However, this method takes a long time and costs too much. So in this paper, the layout optimization of exhibits is considered to reduce congestion as shown in Fig.1. By changing the layout of exhibits, the congestion will be reduced. In previous researches, the relationship between layout and human behavior in exhibition space has been investigated in [1], [2] and [3].

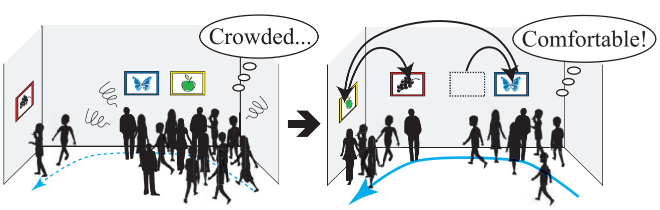

Fig. 1. Congestion reduction by the layout optimization of exhibits

This research was supported by the "Research on Macro/Micro Modeling of Human Behavior in the Swarm and Its Control" under the Core Research for Evolutional Science and Technology (CREST) Program (Research area : Advanced Integrated Sensing Technologies), Japan Science and Technology Agency (JST).

M. Okada, Y. Motegi and K. Yamamoto are with the Department of Mechanical Sciences and Engineering, Tokyo Institute of Technology, 2-12-1 Oookayama Meguro-ku Tokyo, 152-8552 JAPAN
okada@mep.titech.ac.jp
motegi.y.ac@m.titech.ac.jp
yamamoto@micro.mep.titech.ac.jp

Because congestion depends on human flow in the space, it is necessary to model it quantitatively to solve the problem. So far, various modeling techniques have been proposed. In [4], [5], and [6], cellar automaton models are proposed. These are the discrete meshed models used for modeling complex phenomena extensively. However, it is difficult to represent people and obstacles accurately using this model because a space is approximated by grids. In [7], people evacuating from building are modeled by stochastically, and optimization of crowd guidance based on probability is contributed. However, because a layout of exhibits is determinable, it is difficult to introduce this model in our situation. In [8], [9] and [10], physically based model of human crowd behavior in panic situations is proposed. Individual behavior is represented by dynamics based on desired velocity. Especially in [10], though individual characteristics are modeled by some parameters which influence desired velocity with time function, the proposed individuality is specialized to evacuees. In addition, because viewing time of visitors varies from individual to individual, it is difficult to represent them using desired velocity. In [11], human swarm is modeled by continuum fluid and its behavior is represented by dynamics based on two-dimensional flow field. Using this model, the space design method is proposed to reduce the congestion using static elements. However, people stopping to view exhibits are difficult to represent only by this two-dimensional model.

In this paper, human behavior is modeled by dynamics including collision avoidance of individuals, and individual characteristics in measured data and viewing behavior are modeled by multi-dimensional extension of dynamics. Furthermore, to design amenity space without congestion, positions of exhibits are optimized by minimizing collision avoidance vector of individuals. This vector causes congestion in the space and the minimization of it enable the satisfaction of viewing exhibits. In the following sections, the human swarm model is proposed and evaluated by simulations, and the layout optimization of exhibits is proposed and verified by experiments using swarm robots which consist of autonomous mobile robots and radio controlled robots.

II. HUMAN SWARM MODELING IN EXHIBITION SPACE

A. *Vector field design and individual behavior*

In this section, the modeling method of human behavior is illustrated. Human intent is represented by vector field based on the measured trajectory, and multidimensional extension of dynamics is introduced to represent individual walking variability and visitors' stopping to view exhibits.

Step 1 The human trajectories in the space (without exhibits) are measured as:

$$\Xi = \{\ \boldsymbol{\xi}_1 \quad \boldsymbol{\xi}_2 \quad \cdots \quad \boldsymbol{\xi}_n\ \} \tag{1}$$

and vector field $\boldsymbol{f}(\boldsymbol{x})$ is designed so that the dynamics represented by

$$\boldsymbol{x}[k+1] = \boldsymbol{x}[k] + \boldsymbol{f}(\boldsymbol{x}[k]) \tag{2}$$

is entrained to Ξ. By setting many $\boldsymbol{x}_k$ near $\boldsymbol{\xi}_k$, $\boldsymbol{f}(\boldsymbol{x}_k)$ is defined by $\boldsymbol{f}(\boldsymbol{x}_k) = \boldsymbol{\xi}_{k+1} - \boldsymbol{x}_k$, and $\boldsymbol{f}(\boldsymbol{x})$ is obtained by functional approximation as shown in Fig.2. In this paper, we use ℓ-th order power polynomial of $\boldsymbol{x}$ as:

$$\boldsymbol{f}(\boldsymbol{x}) = \boldsymbol{a}_0 + \boldsymbol{a}_1\boldsymbol{x} + \boldsymbol{a}_2\boldsymbol{x}^2 + \cdots + \boldsymbol{a}_\ell\boldsymbol{x}^\ell \tag{3}$$

$$\boldsymbol{x} = \left[\ x \quad y\ \right]^T \tag{4}$$

where $\boldsymbol{a}_i$ are coefficients of polynomial. Note that $\boldsymbol{x}^n$ is defined by

$$\boldsymbol{x}^n = \left[\ x^n \quad x^{n-1}y \quad \cdots \quad xy^{n-1} \quad y^n\ \right]^T \tag{5}$$

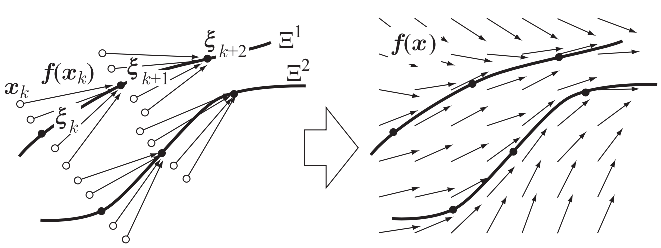

Fig. 2. Definition of vector field

Step 2 Individual behavior is defined by

$$\boldsymbol{x}[k+1] = \boldsymbol{x}[k] + \boldsymbol{f}(\boldsymbol{x}[k]) + \sum_{j\neq i}\boldsymbol{v}^{ij} + \sum_{w}\boldsymbol{v}_w \tag{6}$$

where $\boldsymbol{v}^{ij}$ and $\boldsymbol{v}_w$ represent collision avoidance vectors with individuals and walls respectively. They are defined by the following equations.

$$\boldsymbol{v}^{ij} = \frac{\gamma_r}{1+\exp\{\alpha_r(\|\boldsymbol{r}^{ij}\| - \beta_r)\}}\frac{\boldsymbol{r}^{ij}}{\|\boldsymbol{r}^{ij}\|} \tag{7}$$

$$\boldsymbol{r}^{ij} = \boldsymbol{x}^i - \boldsymbol{x}^j \tag{8}$$

where α_r, β_r and γ_r are constants. $\boldsymbol{v}_w$ is defined in a similar way.

B. Modeling of individual characteristics in measured data

Because $\boldsymbol{f}(\boldsymbol{x})$ is a smooth function that is the macro model of human swarm representing human intent, individual behavior does not always follow the measured route Ξ. There is error between Ξ and $\boldsymbol{f}(\boldsymbol{x})$ as:

$$\boldsymbol{\delta}_k = (\boldsymbol{\xi}_{k+1} - \boldsymbol{\xi}_k) - \boldsymbol{f}(\boldsymbol{\xi}_k) \tag{9}$$

Because Ξ includes walking variety, $\boldsymbol{\delta}_k$ can be considered as individual characteristics. In this paper, $\boldsymbol{\delta}_k$ is modeled by dynamics as follows:

$$\begin{aligned}\boldsymbol{\delta}[k] &= c_{x0} + c_{x1}\boldsymbol{x}[k] + c_{x2}\boldsymbol{x}^2[k] + \cdots + c_{x\ell}\boldsymbol{x}^\ell[k] \\ &\quad + c_{d0} + c_{d1}\boldsymbol{d}[k] + c_{d2}\boldsymbol{d}^2[k] + \cdots + c_{d\ell}\boldsymbol{d}^\ell[k]\end{aligned} \tag{10}$$

$$\boldsymbol{d}[k] = \left[\ \boldsymbol{\delta}^T[k-1] \quad \cdots \quad \boldsymbol{\delta}^T[k-m]\ \right]^T \in R^{2m} \tag{11}$$

where m is the number of past errors which is determined based on "False Nearest Neighbor (FNN)" method [12]. m is obtained by the smallest integer that satisfies the following inequality.

$$\min_{i\neq j}\|\boldsymbol{d}[i] - \boldsymbol{d}[j]\| > r_m \tag{12}$$

where r_m is a threshold of distance.

Because of large m, the calculation cost in (10) will be high, and dimensional reduction is required. To hold the effectiveness of FNN, the following Principal Component Analysis is utilized. Consider the linear projection T that reduces $\boldsymbol{d}$ to $\widehat{\boldsymbol{d}}$ as follows.

$$\widehat{\boldsymbol{d}} = T\boldsymbol{d} \tag{13}$$

Then, we can obtain T that maximizes the distance $\Delta(\widehat{\boldsymbol{d}}^{ij})$

$$\Delta(\widehat{\boldsymbol{d}}^{ij}) = \frac{\widehat{\boldsymbol{d}}[i] - \widehat{\boldsymbol{d}}[j]}{\|\widehat{\boldsymbol{d}}[i] - \widehat{\boldsymbol{d}}[j]\|} \quad (i \neq j) \tag{14}$$

by using Singular Value Decomposition (SVD) of the following matrix.

$$\Delta_D = \left[\ \Delta(\boldsymbol{d}^{12}) \quad \Delta(\boldsymbol{d}^{13}) \quad \cdots\ \right] \tag{15}$$

SVD of Δ_D is represented by

$$\begin{aligned}\Delta_D &= USV^T \\ &= \left[\ U_1 \quad U_2\ \right]\begin{bmatrix} S_1 & 0 \\ 0 & S_2\end{bmatrix}\begin{bmatrix} V_1^T \\ V_2^T\end{bmatrix}\end{aligned} \tag{16}$$

$$S_1 = \mathrm{diag}\{\ \sigma_1 \quad \sigma_2 \quad \cdots \quad \sigma_{r_d}\ \} \tag{17}$$

$$S_2 = \mathrm{diag}\{\ \sigma_{r_d+1} \quad \sigma_{r_d+2} \quad \cdots \quad \sigma_{2m}\ \} \tag{18}$$

By assuming $\sigma_{r_d} \gg \sigma_{r_d+1}$, the linear projection T is obtained by

$$T = U_1^T \tag{19}$$

By using the reduced $\widehat{\boldsymbol{d}}$, equation (10) is rewritten by

$$\begin{aligned}\boldsymbol{\delta}[k] &= c_{x0} + c_{x1}\boldsymbol{x}[k] + c_{x2}\boldsymbol{x}^2[k] + \cdots + c_{x\ell}\boldsymbol{x}^\ell[k] \\ &\quad + c_{d0} + c_{d1}\widehat{\boldsymbol{d}}[k] + c_{d2}\widehat{\boldsymbol{d}}^2[k] + \cdots + c_{d\ell}\widehat{\boldsymbol{d}}^\ell[k]\end{aligned} \tag{20}$$

and equation (6) is replaced by

$$\boldsymbol{x}[k+1] = \boldsymbol{x}[k] + \boldsymbol{f}(\boldsymbol{x}[k]) + \sum_{j\neq i}\boldsymbol{v}^{ij} + \sum_{w}\boldsymbol{v}_w + \boldsymbol{\delta}[k] \tag{21}$$

Individual behavior based on (6) and (21) are compared by the simulation as shown in Fig.3. In (a) and (b), black circles show trajectories of three individuals based on (6) and (21) respectively. The entrance is the upper left corner and the exit is the lower right corner. Black lines and blue lines represent walls and human routes Ξ. Because individuals behave along human routes in (b), we can say that the proposed model based on (21) represents individual walking variability.

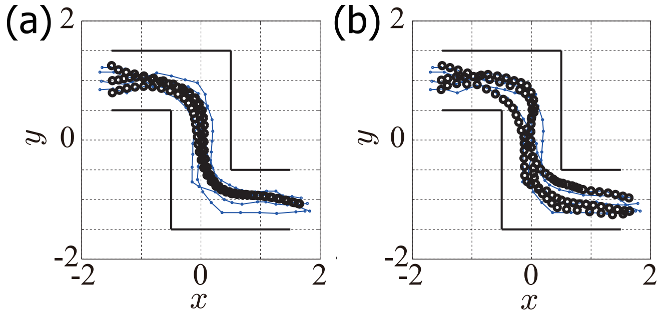

Fig. 3. Trajectories of three individuals based on the proposed model

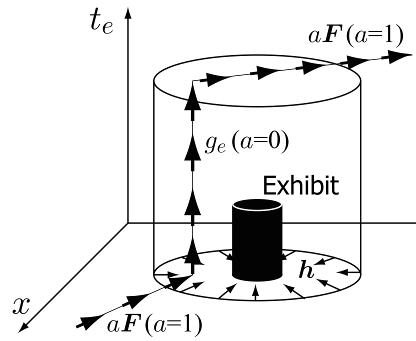

Fig. 4. Individual behavior based on the proposed model

C. Multi-dimensional extension of dynamics for human stop modeling

People in the exhibition space will stop to view exhibits, however, it is difficult to represent stopping behavior by two-dimensional vector field $\boldsymbol{f}(\boldsymbol{x})$. In this section, by introducing the viewing coordinate t_e for each exhibit e, viewing behavior is modeled by multi-dimensional extension of dynamics. The individual behavior is redefined as:

$$\boldsymbol{x}[k+1] = \boldsymbol{x}[k] + a\boldsymbol{F} \tag{22}$$

$$t_e[k+1] = t_e[k] + bg_e(\boldsymbol{x}, t_e) \tag{23}$$

$$\boldsymbol{F}(\boldsymbol{x}, t_e) = \boldsymbol{f}(\boldsymbol{x}) + \sum_{j \neq i} \boldsymbol{v}^{ij} + \sum_{w} \boldsymbol{v}_w + \boldsymbol{\delta} + \boldsymbol{h}(\boldsymbol{x}, t_e) \tag{24}$$

a is a variable that is defined by

$$a = \begin{cases} \sqrt{\dfrac{\|\boldsymbol{F}\|^2 - \|\boldsymbol{G}\|^2}{\|\boldsymbol{F}\|^2}} & (\|\boldsymbol{F}\| \geq \|\boldsymbol{G}\|) \\ 0 & (\|\boldsymbol{F}\| < \|\boldsymbol{G}\|) \end{cases} \tag{25}$$

$$\boldsymbol{G} = \left[\begin{array}{ccc} g_1(\boldsymbol{x}, t_1) & \cdots & g_E(\boldsymbol{x}, t_E) \end{array}\right]^T \tag{26}$$

where E is the number of exhibits. b is a constant varying from individual to individual. Functions g_e and $\boldsymbol{h}$ are defined as follows respectively.

$$g_e(\boldsymbol{x}, t_e) = \frac{\gamma_g S_e}{1 + \exp\{-\alpha_g(\|\boldsymbol{r}_e\| - \beta_g)\}} \tag{27}$$

$$\boldsymbol{h}(\boldsymbol{x}, t_e) = \sum_{e=1}^{r} \gamma_h S_e \exp(-\alpha_h \|\boldsymbol{r}_e\|^2) \frac{\boldsymbol{r}_e}{\|\boldsymbol{r}_e\|} \tag{28}$$

$$S_e = \frac{1}{1 + \exp\{\alpha_e(t_e - \beta_e)\}} \tag{29}$$

$$\boldsymbol{r}_e = \boldsymbol{x}_e - \boldsymbol{x} \tag{30}$$

where α_*, β_* and γ_* are constants and $\boldsymbol{x}_e$ denotes the position of exhibit e. The constants are identified on the basis of observation of human behavior in a real exhibition space. g_e represents the velocity along t_e axis and $\boldsymbol{h}$ represents the attraction to exhibit. Note that norm of $\boldsymbol{F}$ is limited as follows:

$$\|\boldsymbol{F}(\boldsymbol{x}, t_e)\| \leq \|\boldsymbol{f}(\boldsymbol{x})\| \tag{31}$$

to prevent the individuals from moving with over velocity. The behavior of individuals using the proposed model is represented by Fig.4. An individual near the exhibit is attracted by $\boldsymbol{h}$. According to (25), a changes to zero and an individual moves along t_e axis, which represents the viewing (stopping behavior) of the individual. After t_e reaches to β_e, a returns to one and an individual moves by following $\boldsymbol{f}(\boldsymbol{x})$. This model can represent visitor's stopping in $\boldsymbol{x}$-space. Fig.5 shows the simulation result of individual behavior in the same exhibition space as Fig.3. Black circles, black lines and blue lines represent individual trajectory, walls and human routes Ξ respectively. Fig.5-(b) shows the projection of individual behavior in Fig.5-(a) to $\boldsymbol{x}$-plane. From this result, we can see that the proposed model represents visitors' stopping to view exhibits by multi-dimensional extension of dynamics.

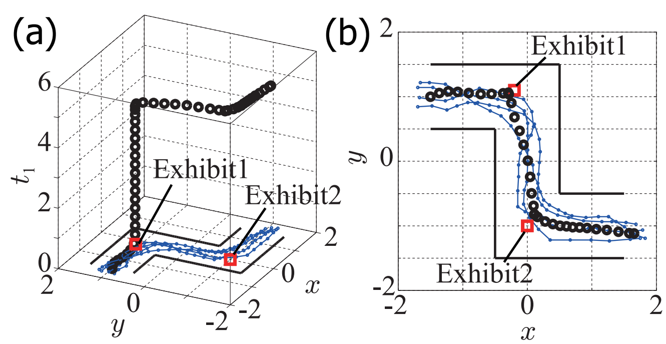

Fig. 5. A trajectory of individual based on the proposed model

III. LAYOUT OPTIMIZATION OF EXHIBITS

Due to congestion, people are not satisfied with viewing exhibits. The cause of congestion is collision avoidance vector of individuals $\boldsymbol{v}^{ij}$. In this section, a layout of exhibits is optimized by minimizing $\boldsymbol{v}^{ij}$ and congestion is reduced. The measured velocity of individual i is represented by

$$\boldsymbol{V}^i = \boldsymbol{\eta}^i[k] - \boldsymbol{\eta}^i[k-1] \tag{32}$$

On the other hand, the ideal velocity is described by

$$\widehat{\boldsymbol{V}}^i = a^i \left\{ \boldsymbol{f}(\boldsymbol{x}^i[k]) + \sum_{w} \boldsymbol{v}_w + \boldsymbol{h}^i(\boldsymbol{x}^i[k], t_e^i[k]) \right\} \tag{33}$$

without $\boldsymbol{v}^{ij}$. By using (32) and (33), the evaluation function J is defined as follow:

$$J = \sum_{i=1}^{N} \left\| \boldsymbol{V}^{i} - \widehat{\boldsymbol{V}}^{i} \right\|^{2} \tag{34}$$

By minimizing J, individual behavior is close to ideal one. Because $\widehat{\boldsymbol{V}}^{i}$ including $\boldsymbol{h}^{i}$ is the function of $\boldsymbol{x}_e$ according to (28) and (30), the partial differential of J with respect to $\boldsymbol{x}_e$ is written by

$$\frac{\partial J}{\partial \boldsymbol{x}_e} = \sum_{i=1}^{N} \frac{2a^{i}H}{\|\boldsymbol{r}_e^{i}\|} \boldsymbol{J}^{iT} \left\{ \left(2\alpha_h + \frac{1}{\|\boldsymbol{r}_e^{i}\|^{2}} \right) \boldsymbol{r}_e^{i} \boldsymbol{r}_e^{iT} - I \right\} \tag{35}$$

$$H = \gamma_h S_e \exp(-\alpha_h \|\boldsymbol{r}_e^{i}\|^{2}) \tag{36}$$

while the partial differential of J with respect to time is defined by

$$\frac{\partial J}{\partial t} = J[k] - J[k-1] \tag{37}$$

By using gradient method, positions of exhibits are updated and optimized as follow:

$$\boldsymbol{x}_e[k+1] = \boldsymbol{x}_e[k] - \frac{\partial J}{\partial t} \left(\frac{\partial J}{\partial \boldsymbol{x}_e} \right)^{T} \Delta x \tag{38}$$

where Δx is a constant. Fig.6 shows the results of the layout optimization of exhibits in the same exhibition space as Fig.5. (a) shows the layout before the optimization and (b) shows after that. The red dashed lines denote trajectories of exhibits in (b). Fig.7 shows time variation of evaluation function J and the number of individuals N from beginning of the optimization. From these figures, we can see that the number of individuals N is reduced by decreasing the evaluation function J which means congestion is reduced. Because the exhibits placed in the middle of the hallway can be watched from any direction, huge crowds do not exist around them. Fig.8 shows distribution and average of the 100 individuals' total time from the entrance to the exit. (a) shows before the optimization and (b) shows after that. Fig.9 and 10 show distribution and averages of the viewing time before and after the optimization. These results show that the average of the viewing time becomes longer by the optimization. Individuals are more satisfied with viewing exhibits because of the longer viewing time in spite of the shorter visit.

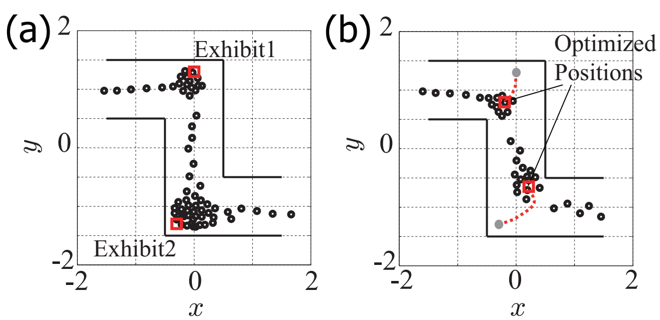

Fig. 6. The simulation result of the layout optimization of exhibits

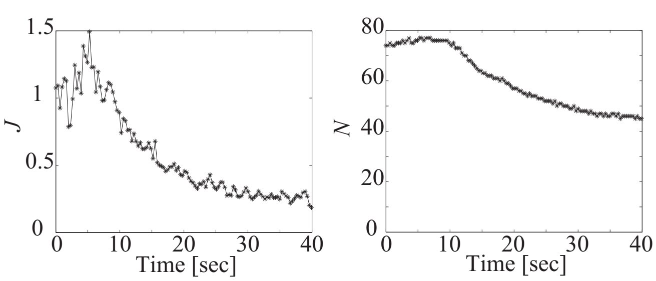

Fig. 7. Time variation of evaluation function and number of individuals in the exhibition space

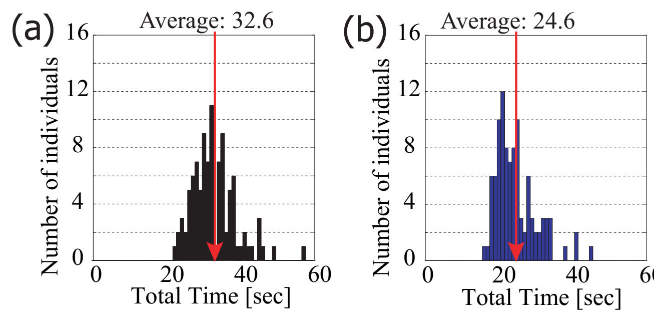

Fig. 8. Distribution of the total time (100 individuals)

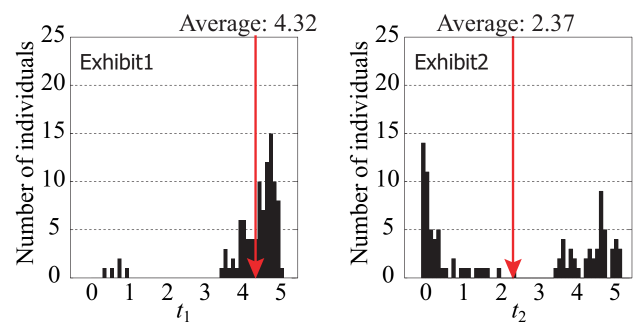

Fig. 9. Distribution of the viewing time BEFORE the layout optimization of exhibits (100 individuals)

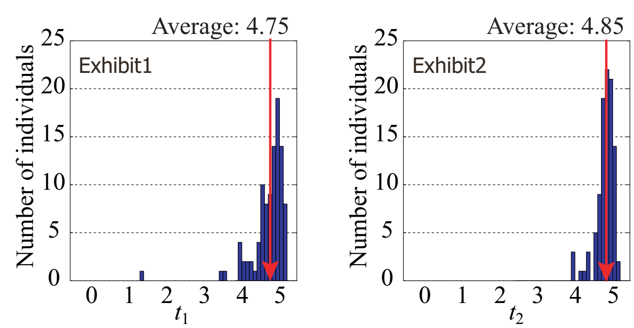

Fig. 10. Distribution of the viewing time AFTER the layout optimization of exhibits (100 individuals)

IV. EXPERIMENTAL VERIFICATION USING SWARM ROBOTS

A. Experimental Mobile Robots

In this section, the proposed method of optimization is verified by experiments using swarm robots in the small

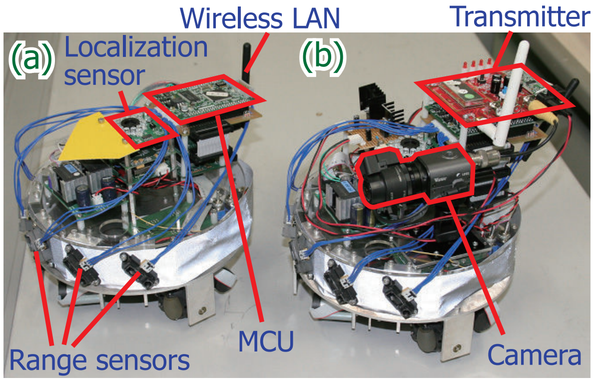

Fig. 11. Autonomous mobile robot and radio control robot

exhibition space. Swarm robots consist of autonomously mobile robots and radio controlled robots. By mixing radio controlled robots, the pseudo human environment is represented. Fig.11-(a) shows an autonomous mobile robot. This robot has a battery, a micro control unit (MCU), a localization sensor and range sensors. Through wireless LAN, robots communicate with host computer. Three omnidirectional wheels are installed in the lower layer. Fig.11-(b) shows a radio control robot which has a camera and a transmitter sending video signal by wireless so that a driver can control the robot with camera images.

B. Experimental Procedure

First, some people control one robot in turns and their trajectories are measured in order to design vector field. Second, the layout of exhibits is optimized by the proposed method. Finally, the total time and the viewing time before and after optimization are compared.

Autonomous mobile robots behave based on the proposed model represented by (22) and (23). Because processing ability of MCU is limited, host computer calculate $\boldsymbol{f}(\boldsymbol{x})$, $\boldsymbol{\delta}$, t_e, $\boldsymbol{h}$ and $\boldsymbol{v}_w$, and velocity commands are sent by wireless LAN. Meanwhile, collision avoidance vector between individuals $\boldsymbol{v}^{ij}$ is calculated by MCU using range sensors information.

C. Experimental Results and Verification

Fig.12 shows robot trajectories (indicated by blue lines) and designed vector field (indicated by green arrows).

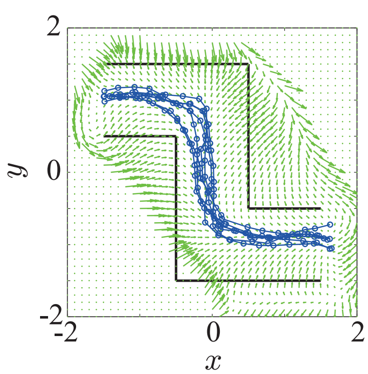

Fig. 12. Designed vector field based on the experimental data

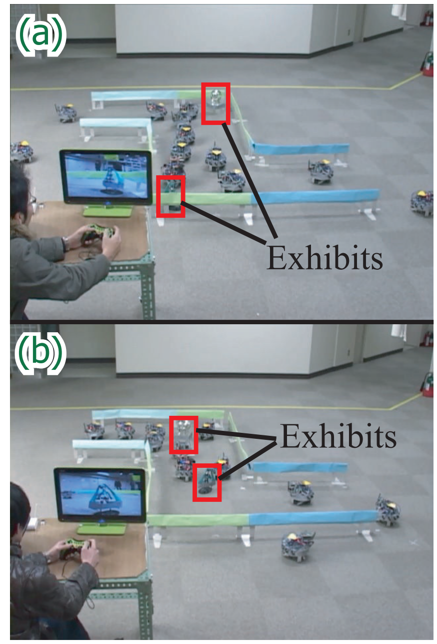

Fig. 13. Overhead view of the experiment using swarm robots

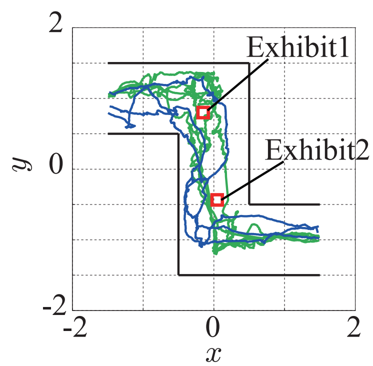

Fig. 14. Trajectories of swarm robots

The layout of two exhibits are optimized by the proposed method in this space. Fig.13 and the attached movie show the experimental environment. In Fig.13-(a) and (b), the layout of exhibits is unoptimized and optimized respectively. The positions of exhibits are indicated by red rectangles. Eleven autonomous mobile robots and one radio controlled robot are used. Some trajectories of radio control robots and autonomous mobile robots are shown in Fig.14. The former is indicated by blue lines and the latter is indicated by green lines. This result shows that the proposed model represents human behavior in exhibition space because the behavior of autonomous mobile robots are mostly consistent with that of radio control robots. As with simulation, distribution and average of the total time of swarm robots are shown in Fig.15. (a) shows before the optimization and (b) shows after that. Red arrows indicate averages of the total time of autonomous mobile robots and blue arrows indicate those of radio control robots. In these results, the layout optimization shorten the average of the total time. In addition, Fig.16 and Fig.17 show distribution and average of the viewing time of swarm robots. In these results, robots are more satisfied with viewing exhibits by the optimization, despite the shorter visit. Consequently, these results show that the proposed optimization method designs the comfortable exhibition space.

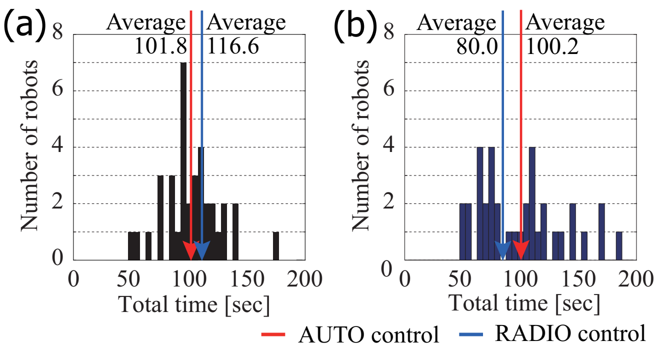

Fig. 15. Distribution of the total time in experiments

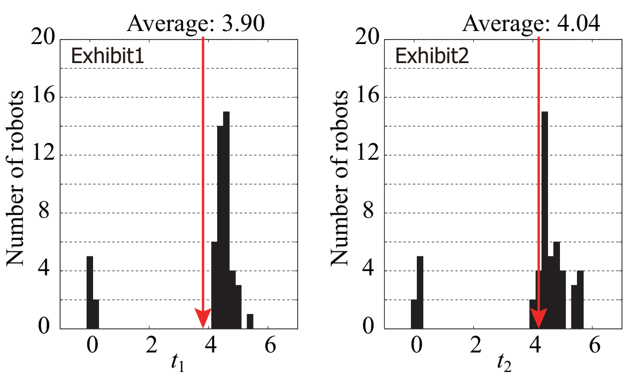

Fig. 16. Distribution of the viewing time in experiments BEFORE the layout optimization of exhibits

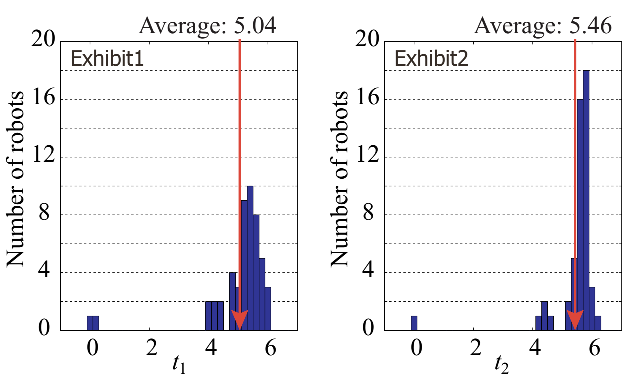

Fig. 17. Distribution of the viewing time in experiments AFTER the layout optimization of exhibits

V. CONCLUSION

In this paper, the macro model of human swarm behavior in exhibition space was proposed, and amenity space was designed by optimizing layout of exhibits. The results of this paper are described as follows:

- Human intent was modeled by two-dimensional vector field, and individual behavior was represented by dynamics including collision avoidance vector of individuals.
- To represent individual characteristics in measured data and visitors' viewing exhibits, multi-dimensional extension of dynamics was introduced. The proposed model was verified by simulations. Individual behavior along with human route and viewing the exhibits was realized.
- The layout optimization of exhibits was proposed by minimizing collision avoidance vector of individuals.
- The proposed optimization method was verified by the simulation and the experiment using swarm robots. The results showed that people took longer viewing time and were more satisfied with viewing exhibits by the optimization, which represent the amenity space was designed.

Congestion exists not only an exhibition space but also an entrance of stations or stadiums. Human behavior in such places is also represented by the proposed model. Furthermore, it will be possible to reduce the congestion using that model.

REFERENCES

[1] M.L. Harvey, R.J. Loomis, P.A. Bell, and M. Marino. The influence of museum exhibit design on immersion and psychological flow. *Environment and Behavior*, Vol. 30, No. 5, pp. 601–627, 1998.

[2] Y.K. Choi. The morphology of exploration and encounter in museum layouts. *Environment and Planning B: Planning and Design*, Vol. 26, pp. 241–250, 1999.

[3] J. Peponis, C. Dalton, J. Wineman, and N. Dalton. Measuring the effects of layout upon visitors' spatial behaviors in open plan exhibition settings. *Environment and Planning B: Planning and Design*, Vol. 31, pp. 453–473, 2004.

[4] S.H.Lee, J.H.Park, and H.K.Pak. Jamming transition in three types of competing pedestrians (adults, children and injured people) with morality, using a cellular automaton model. *the Korean Physical Society*, Vol. 44, No. 3, pp. 660–663, 2004.

[5] J. Was. Cellular automata model of pedestrian dynamics for normal and evacuation conditions. In *Proceedings of 5th International Conference on Intelligent Systems Design and Applications*, pp. 154–159, 2005.

[6] W. G. Weng, T. Chen, H. Y. Yuan, and W. C. Fan. Cellular automaton simulation of pedestrian counter flow with different walk velocities. *Phys. Rev. E*, Vol. 74, No. 3, p. 036102, 2006.

[7] P. Wang, P.B. Luh, S.C. Chang, and J. Sun. Modeling and optimization of crowd guidance for building emergency evacuation. In *Proceedings of 4th IEEE Conference on Automation Science and Engineering*, pp. 328–334, 2008.

[8] D. Helbing, I. Farkas, and T. Vicsek. Simulating dynamical features of escape panic. *Nature*, Vol. 407, pp. 487–490, 2000.

[9] N. Pelechano and N.I. Badler. Modeling crowd and trained leader behavior during building evacuation. *IEEE Computer Graphics and Applications*, Vol. 26, pp. 80–86, 2006.

[10] Adriana Braun, Soraia R. Musse, Luiz P. L. de Oliveira, and Bardo E. J. Bodmann. Modeling individual behaviors in crowd simulation. *Computer Animation and Social Agents, International Conference on*, Vol. 0, p. 143, 2003.

[11] M. Okada and Y. Homma. Amenity design for congestion reduction based on continuum model of swarm. In *Proceedings of 13th International Conference on Mechatronics Technology*, 2009.

[12] Matthew B. Kennel, Reggie Brown, and Henry D. I. Abarbanel. Determining embedding dimension for phase-space reconstruction using a geometrical construction. *Phys. Rev. A*, Vol. 45, No. 6, pp. 3403–3411, 1992.